ANTIMICROBIAL AGENTS AND CHEMOTHERAPY, Dec. 2009, p. 4979–4986 Vol. 53, No. 12
0066-4804/09/$12.00 doi:10.1128/AAC.00497-09

Atomic Force Microscopy Investigation of the Morphology and Topography of Colistin-Heteroresistant *Acinetobacter baumannii* Strains as a Function of Growth Phase and in Response to Colistin Treatment▽

Rachel L. Soon,[1] Roger L. Nation,[1] Patrick G. Hartley,[2] Ian Larson,[3]†* and Jian Li[1]†*

Facility for Anti-Infective Drug Development and Innovation[1] and Drug Delivery, Disposition and Dynamics,[3] Monash Institute of Pharmaceutical Sciences, Monash University, 381 Royal Parade, Parkville, Victoria 3052, Australia, and CSIRO Molecular and Health Technologies, Ian Wark Laboratory, Bayview Ave., Clayton, Victoria 3169 Australia[2]

Received 16 April 2009/Returned for modification 5 July 2009/Accepted 21 September 2009

The prevalence of infections caused by multidrug-resistant gram-negative *Acinetobacter baumannii* strains and the lack of novel antibiotics under development are posing a global dilemma, forcing a resurgence of the last-line antibiotic colistin. Our aim was to use atomic force microscopy (AFM) to investigate the morphology and topography of paired colistin-susceptible and -resistant cells from colistin-heteroresistant *A. baumannii* strains as a function of bacterial growth phase and colistin exposure. An optimal AFM bacterial sample preparation protocol was established and applied to examine three paired strains. Images revealed rod-shaped colistin-susceptible cells (1.65 ± 0.27 μm by 0.98 ± 0.07 μm) at mid-logarithmic phase, in contrast to spherical colistin-resistant cells (1.03 ± 0.09 μm); the latter were also more diverse in appearance and exhibited a rougher surface topography (7.05 ± 1.3 nm versus 11.4 ± 2.5 nm for susceptible versus resistant, respectively). Cellular elongation up to ~18 μm at stationary phase was more commonly observed in susceptible strains, although these "worm-like" cells were also observed occasionally in the resistant population. The effects of colistin exposure on the cell surface of colistin-susceptible and -resistant cells were found to be similar; topographical changes were minor in response to 0.5 μg/ml colistin; however, at 4 μg/ml colistin, a significant degree of surface disruption was detected. At 32 μg/ml colistin, cellular clumping and surface smoothening were evident. Our study has demonstrated for the first time substantial morphological and topographical differences between colistin-susceptible and -resistant cells from heteroresistant *A. baumannii* strains. These results contribute to an understanding of colistin action and resistance in regard to this problematic pathogen.

The rapid emergence of infections caused by multidrug-resistant (MDR) bacteria, coupled with a significant decline in antibiotic discovery and development, is posing a considerable public health threat worldwide. Gram-negative bacteria such as *Acinetobacter baumannii*, *Pseudomonas aeruginosa*, and *Klebsiella pneumoniae* continue to prove problematic, with few novel antibiotics currently in the drug development pipeline (4). *A. baumannii*, in particular, is presenting increasing cause for concern with resilience demonstrated by its ability to survive for prolonged periods at various temperatures, pHs, and nutrient-limiting conditions, thus enabling rapid nosocomial spread, particularly in critically ill and immunocompromised patients (2). Management of infections caused by *A. baumannii* is complicated by the emergence of strains that are resistant to almost all available antibiotics (25).

In an era of increasing prevalence of MDR *A. baumannii* strains, interest in the polymyxin class of antibiotics stems from their significant activity against gram-negative MDR organisms and current low levels of resistance (26). Two major polymyxins, colistin (also known as polymyxin E) and polymyxin B, differing by a single amino acid, have been employed clinically as last-line therapy against infections caused by MDR gram-negative bacteria, including *A. baumannii* (13, 23, 26, 46). While the exact mechanism of action of colistin is yet to be completely elucidated, there is strong evidence to indicate that the primary target is the gram-negative outer membrane, whereby electrostatic forces mediate the initial interaction between the cationic polymyxin and negatively charged lipopolysaccharide (LPS) (18). Subsequently, hydrophobic interactions enable polymyxin to insert into the lipid membrane (18). Recent reports of both colistin-resistant and colistin-heteroresistant *A. baumannii* strains (defined as the presence of a small subpopulation of resistant bacteria within a strain that is susceptible based on MICs) (19, 27) serve to emphasize the growing concerns presented by this pathogen. Rapid emergence of colistin resistance has also been noted following colistin exposure both in vitro (38) and in vivo (19).

It has been demonstrated that phase of growth is a determinant of the hydrophobicity and surface charge of the bacterial outer membrane (17, 41), and accordingly, growth phase has the potential to influence the interaction between colistin and the outer membrane. Interestingly, a significant decrease in colistin susceptibility of *A. baumannii* at stationary phase in

* Corresponding author. Mailing address: Facility for Anti-Infective Drug Development and Innovation, Drug Delivery, Disposition and Dynamics, Monash Institute of Pharmaceutical Sciences, Monash University, 381 Royal Parade, Parkville, Victoria 3052, Australia. Phone for J. Li: 61 3 9903 9702. Fax: 61 3 9903 9629. E-mail: Jian.Li@pharm.monash.edu.au. Phone for I. Larson: 61 3 9903 9570. Fax: 61 3 9903 9629. E-mail: Ian.Larson@pharm.monash.edu.au.

† I. Larson and J. Li are joint senior authors.

▽ Published ahead of print on 28 September 2009.

comparison to exponential phase was discovered recently (33). Despite these findings, the morphology and topography of *A. baumannii* at different growth phases and the effect of colistin treatment on colistin-susceptible versus -resistant subpopulations within clinical heteroresistant strains have yet to be characterized. The aim of the present investigation was therefore to explore these aspects using atomic force microscopy (AFM), an extraordinarily powerful tool for microbiological investigations (11). We hypothesized that because the LPS of the outer membrane is the initial site of colistin action on gram-negative bacteria (17) and because LPS plays such a crucial role in the integrity of the outer membrane (1), phenotypic differences in regard to surface structure and cell morphology may exist between susceptible and resistant cells.

MATERIALS AND METHODS

Chemicals. A stock solution (1 mg/ml) of colistin (sulfate form, 20,374 U/mg; Zhejiang Shenghua Biok Biology, Co., Ltd., China) was prepared in Milli-Q water (Millipore, Australia) followed by sterilization with 0.22-μm syringe filters (Sartorius, Australia). The colistin solution was stored at 4°C for up to 1 month, conditions under which colistin is stable (unpublished data).

Bacterial strains. Three colistin-heteroresistant strains of *A. baumannii* (clinical strains 9 and 16 and reference strain ATCC 19606 from the American Type Culture Collection, Manassas, VA) were employed. The MICs of colistin were 2 μg/ml for strain 9 and 1 μg/ml for strains 16 and ATCC 19606; all three strains belong to different pulsed-field gel electrophoresis clonotypes (27). From each parent strain a paired colistin-resistant strain (MICs of >128 μg/ml) was obtained, which represented the colistin-resistant subpopulation in each heteroresistant strain (27); these were designated as "Col10" as they were able to grow in the presence of at least 10 μg/ml colistin (see below). Thus, a total of six strains (9, 9 Col10, 16, 16 Col10, ATCC, and ATCC Col10) were examined in this study. Investigation of the effect of colistin treatment was performed on paired colistin-susceptible and -resistant subpopulations of strains 16 and ATCC.

All strains were stored at −80°C. The susceptible parent strains (9, 16, and ATCC) were subsequently subcultured onto nutrient agar plates (Medium Preparation Unit, University of Melbourne, Australia). Cation-adjusted Mueller-Hinton broth was employed for overnight culture, following which early-logarithmic, mid-logarithmic, and stationary-phase cultures were prepared according to the optical density at 600 nm. All broth cultures were incubated at 37°C in an orbital shaker (Thermoline Scientific, Australia). The respective colistin-resistant strains (9 Col10, 16 Col10, and ATCC Col10), obtained from our previous study (27), were prepared in the same manner as their parent colistin-susceptible strains, except that the initial subculture and overnight broth culture were grown in the presence of 10 μg/ml colistin. Early-logarithmic, mid-logarithmic, and stationary-phase cultures of strains 16 Col10 and ATCC Col10 were grown in the absence of colistin to avoid potential structural modifications induced by the antibiotic.

Sample preparation for AFM experiments. To determine the optimal conditions for sample pretreatment, mid-logarithmic cells of ATCC 19606 were harvested from broth culture by centrifugation at 3,000 or 15,000 × *g* for 5 or 15 min at 25°C. Cells were washed up to six times and resuspended in Milli-Q water to prepare final bacterial suspensions containing ~1×10^8 CFU/ml. A 5-μl drop of bacterial suspension was deposited on a clean glass slide and allowed to air dry before imaging. To examine the effect of colistin treatment on *A. baumannii*, colistin (1 mg/ml) was added to 5 ml of bacterial culture to achieve final concentrations of 0.5, 4, and 32 μg/ml. Bacterial broth cultures were incubated at 37°C in an orbital shaker for 20 min; this duration ensured that there were sufficient cells left for AFM imaging after rapid concentration-dependent killing (30). Following centrifugation and washing, a 5-μl drop of bacterial suspension was deposited for AFM imaging, as described above.

AFM imaging and analysis. AFM height, amplitude, and phase images were simultaneously acquired using a Dimension 3000 microscope with a Nanoscope IIIa controller (Digital Instruments, Santa Barbara, CA) operating in tapping mode. Standard tapping mode silicon cantilevers (Tap300 Budget Sensors; Innovative Solutions Bulgaria, Ltd.) were used (125 μm in length, nominal spring constants of 40 N/m, and typical resonant frequencies of 300 kHz). The radius of curvature of the AFM tips was nominally less than 10 nm. A scan rate of 0.5 to 1 Hz was employed at a resolution of 512 pixels per line. Height images were primarily used for quantitative measurements, while amplitude and phase images functioned to present surface features with greater clarity. Surface plots were derived from height data. All images were further processed using the Nanoscope 5.13 software by means of first-order flattening and first-order contrast enhancement. Images were not processed prior to quantitative measurements.

To validate the reproducibility of observations and quantify morphological parameters, multiple images were collected on at least four independently prepared bacterial samples over 2 separate days. Several (three to six) large scans (20 μm by 20 μm) were performed on randomly chosen sections of the glass slides, encompassing at least 100 bacterial cells in total, from which the morphology of the sample bacterial population was determined. High-magnification images (5 μm by 5 μm) were utilized to evaluate cell dimensions. Roughness measurements were conducted over three different 500-nm by 500-nm areas on individual cells. A minimum of 10 cells of each strain were characterized for dimensions and roughness. Analysis of variance and two-sample *t* tests were used to determine the significance of differences in cellular dimensions and surface roughness (Microsoft Excel).

RESULTS

Sample pretreatment. AFM images of *A. baumannii* ATCC 19606 cells, prepared with various centrifugation and washing steps, are presented in Fig. 1. The characteristic rod shape of typical colistin-susceptible *A. baumannii* cells was evident after all washing and centrifugation protocols. The optimum bacterial sample preparation protocol was determined to be two washing steps at a centrifugation speed of 3,000 × *g* for 5 min (Fig. 1C). Fewer washes revealed cells that appeared to be blanketed by an amorphous material (Fig. 1A and B), while more than two washes (Fig. 1D and E) or increased speed (Fig. 1F) or duration (Fig. 1G) of centrifugation did not improve the image quality (Fig. 1D to G) or modify cell surface roughness (data not shown). Washing twice followed by centrifugation at a higher speed of 15,000 × *g* (Fig. 1F), or for a longer duration of 15 min at 3,000 × *g* (Fig. 1G), resulted in an observable shortening of pili in comparison to that shown in Fig. 1C, without dramatic effects on the cellular body. For the remainder of this study, all samples were washed twice with Milli-Q water followed by centrifugation at 3,000 × *g* for 5 min. The adequacy of this protocol was confirmed using all other colistin-susceptible and -resistant strains of *A. baumannii*. Images of cells prepared using this protocol were similar to those of cells which were taken directly from culture on agar plates and dispersed in Milli-Q water without centrifugation (data not shown).

Morphology and topography of colistin-susceptible and -resistant bacterial cells in different growth phases. Representative images of ATCC 19606 and ATCC 19606 Col10 at different growth phases are shown Fig. 2; similar images were captured for the other strains (images not shown). As is evident in Fig. 2, colistin-susceptible cells were rod shaped at all growth phases; at stationary phase, elongated cells, including numerous worm-like cells, were observed. In contrast, colistin-resistant cells exhibited a spherical morphology at early- and mid-logarithmic phases; however, marked cellular heterogeneity was evident in stationary phase with cocci and rod and elongated worm-like cells (Fig. 2). Pili were observed at all growth phases for colistin-susceptible strains but were substantially reduced in number and length for colistin-resistant cells (Fig. 2). In comparison to colistin-susceptible cells, greater topographic variability was noted on colistin-resistant cells, with some presenting with grooves on the exterior (Fig. 2E). Furthermore, resistant cells displayed a finer surface texture

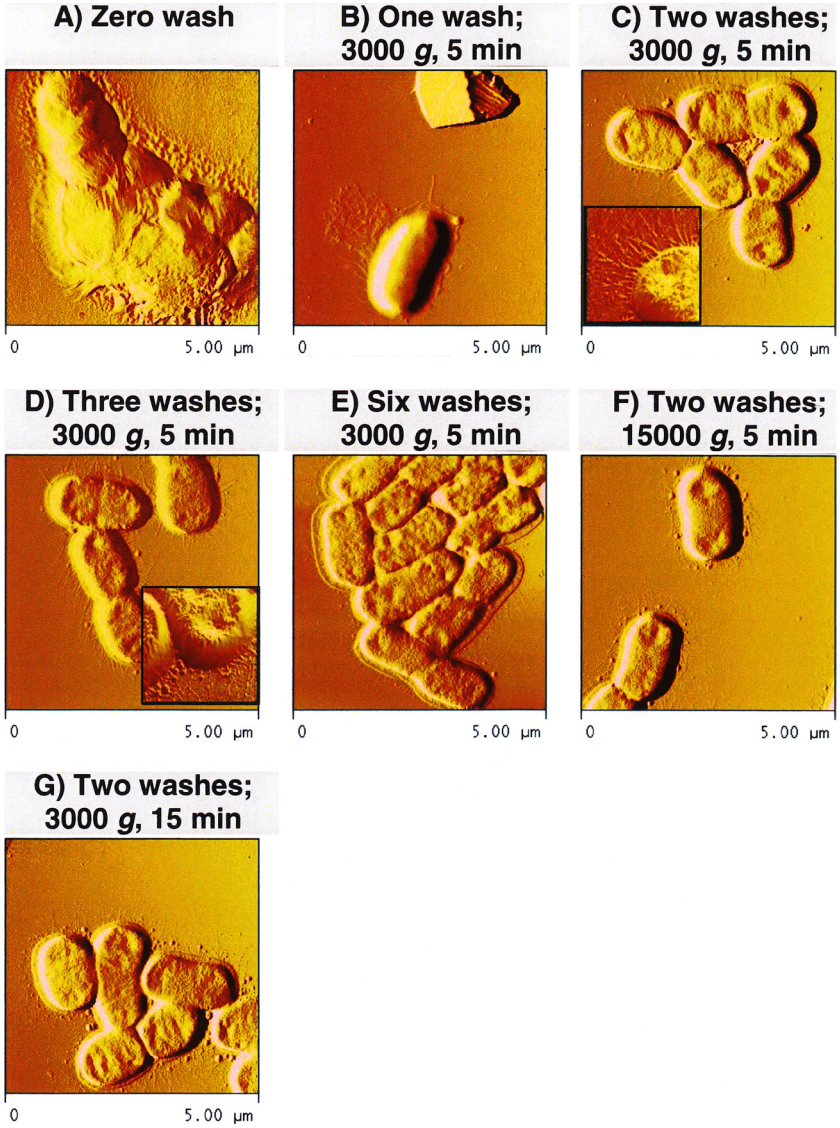

FIG. 1. Influence of sample preparation on AFM amplitude images of *A. baumannii* ATCC 19606. Panels A to G show the influence of the number of washing steps and centrifugation conditions. High-magnification (1 μm by 1 μm) images are displayed within panels C and G to emphasize extracellular appendages (see text).

(Fig. 3). These characteristics were evident across all growth phases.

Bacterial dimensions and surface roughness are summarized in Table 1. Average cellular dimensions at stationary phase were not tabulated due to the marked morphological heterogeneity (Fig. 2C and F). There were no significant differences ($P > 0.05$) in a given cell dimension (i.e., length, width, or diameter) between early- and mid-logarithmic phases for each strain (Table 1). At stationary phase, very elongated cells of up to 18 μm were observed; these cells had similar widths (~1 μm) to susceptible cells at early- and mid-logarithmic phases. The worm-like cells were more prevalent in the susceptible strain (~1 in 8) than in the resistant one (~1 in 25). Surface roughness was invariant across all growth phases ($P > 0.05$); however, significant differences were noted between strains ($P < 0.05$) (Table 1).

Effect of colistin treatment. Representative images of mid-logarithmic-phase (Fig. 4) and stationary-phase (images not shown) ATCC 19606 and ATCC 19606 Col10 cells illustrate the effect of 20 min of exposure to colistin (0.5, 4, and 32 μg/ml). The nature and degree of outer membrane damage caused by colistin treatment of susceptible or resistant cells were found to be similar at both mid-logarithmic (Fig. 4) and stationary growth phases (images not shown) (Table 2).

Damage to the outer membrane of susceptible mid-logarithmic cells was minimal in response to the 0.5-μg/ml treatment (Fig. 4A). Maintenance of cellular shape was accompanied by small pits and indentations across the bacterial surface (Fig. 4A). The surface roughness (8.64 ± 2.4 nm) (Table 2) was not significantly different ($P > 0.05$) from that of untreated cells (7.65 ± 1.7 nm) (Table 1). Substantial topographical changes (numerous grooves and incisions) were observed, together with

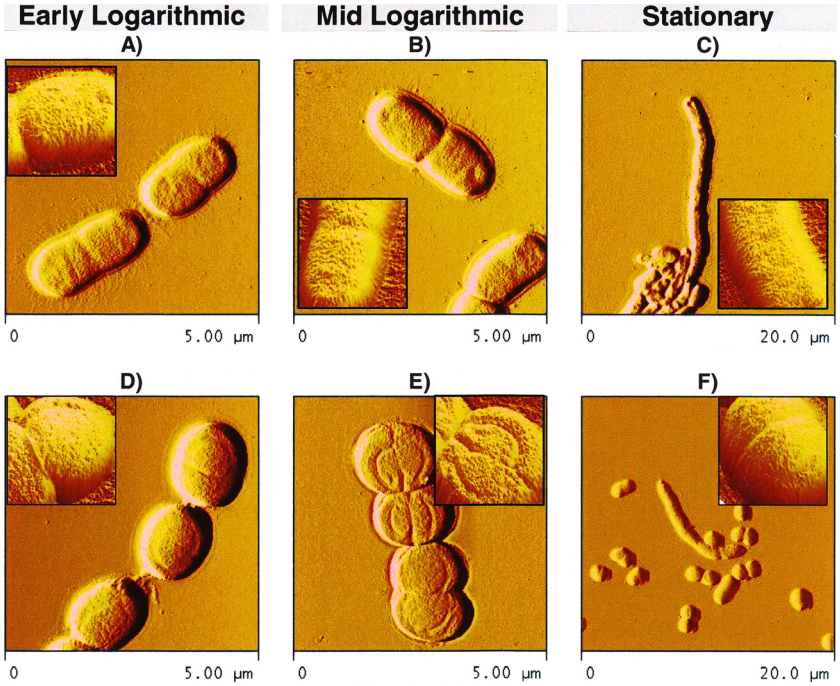

FIG. 2. AFM amplitude images and high-magnification surface three-dimensional plots (1 μm by 1 μm; reconstructed from height data) of colistin-susceptible *A. baumannii* strain ATCC 19606 (A to C) and colistin-resistant strain ATCC Col10 (D to F) in different growth phases.

the presence of debris surrounding some cells upon treatment with 4 μg/ml colistin (Fig. 4B). These alterations were consistent with a significant increase ($P < 0.05$) in surface roughness (13.5 ± 5.6 nm) (Table 2) compared with untreated cells. Surprisingly, images acquired following colistin treatment at 32 μg/ml revealed cells with much smoother topography on visual inspection (Fig. 4C). This apparent smoothness was not reflected by quantitative roughness measurements which indicated an increased surface roughness ($P < 0.05$) (19.8 ± 4.3 nm) (Table 2) in comparison to either untreated cells, or cells treated at lower colistin concentrations. Additionally, the total number of cells present on the slide for imaging was substantially reduced, and the remaining cells displayed a tendency to cluster together rather than scatter as discrete entities (Fig. 4C). Average bacterial dimensions were not affected by colistin exposure at all concentrations ($P > 0.05$) (Table 2).

Changes to the surface of mid-logarithmic-phase colistin-resistant cells were not noticed upon treatment with 0.5 μg/ml colistin (Fig. 4D). Interestingly, surface disruptive effects observed at 4 μg/ml (Fig. 4E) and 32 μg/ml (Fig. 4F) were analogous to those seen with the colistin-susceptible strains (Fig. 4B and C) in response to colistin treatment at the same concentrations. A significant ($P < 0.05$) increase in average roughness (23.8 ± 5.2 nm) (Table 2) was noted after exposure to 4 μg/ml colistin in comparison to untreated cells (11.4 ± 2.0 nm) (Table 1), while treatment with 32 μg/ml colistin revealed

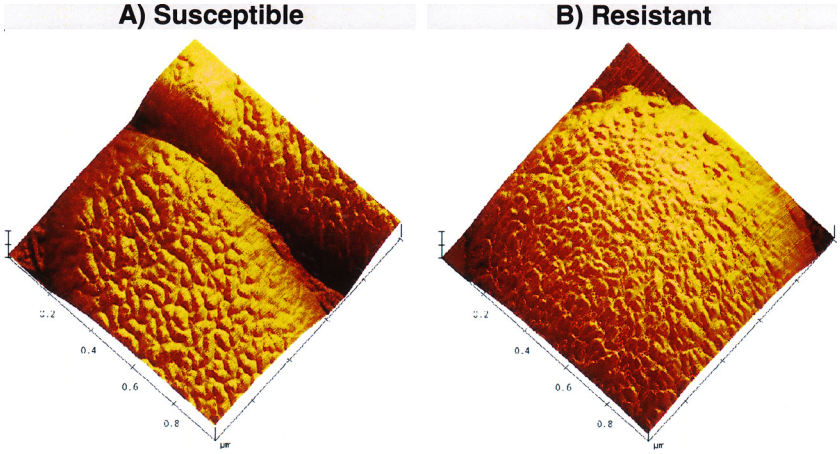

FIG. 3. Surface three-dimensional plot (1 μm by 1 μm; reconstructed from height data) illustrating the topography of colistin-susceptible (A) and -resistant (B) *A. baumannii* ATCC 19606 cells.

TABLE 1. Cellular dimensions and average RMS surface roughness of colistin-susceptible and -resistant (ATCC 19606 Col10) cells of *A. baumannii* ATCC 19606 at different growth phases

Growth phase	Susceptible			Resistant	
	Width (μm)	Length (μm)	Avg RMS surface roughness (nm)	Diam (μm)	Avg RMS surface roughness (nm)
Early log	0.98 ± 0.07[a]	1.65 ± 0.27[a]	7.05 ± 1.3[b,c]	1.03 ± 0.09[a]	11.4 ± 2.5[b,c]
Mid-log	1.03 ± 0.10[a]	1.61 ± 0.21[a]	7.65 ± 1.7[b,c]	0.97 ± 0.11[a]	11.4 ± 2.0[b,c]
Stationary	ND[d]	ND	6.71 ± 1.7[b,c]	ND	11.6 ± 2.3[b,c]

[a] Not significantly different from corresponding dimension across growth phases ($P > 0.05$).
[b] Not significantly different across growth phases ($P > 0.05$).
[c] Significantly different between susceptible and resistant cells for a given growth phase ($P < 0.05$).
[d] ND, not determined due to marked morphological heterogeneity.

cells with a smoother topography (14.3 ± 4.1 nm) (Table 2) and a tendency for clumping to occur (Fig. 4F).

DISCUSSION

The development of antimicrobial resistance phenomena in MDR *A. baumannii* strains has highlighted the urgent requirement to investigate its resistance to the last-line therapy, colistin. In the present study, AFM was utilized to examine differences in the morphology and topography of paired colistin-susceptible and -resistant cells from heteroresistant *A. baumannii* strains and the effect of colistin. Since its advent in 1986, AFM has been credited as a powerful tool for microbiological investigations (11), owing in part to its extended capability to function as both a force-sensing device and as an imaging tool. Based on a principle involving the mechanical scanning of samples without use of lenses, photons, or electrons, the requirement for sample preparation that may potentially alter the native cell is minimized (in comparison to light and electron microscopy), while images with exceptional nanometer resolution and topographic contrast are captured (43). A limited number of *A. baumannii* images have been acquired using electron microscopy (21, 34) and phase-contrast and scanning confocal laser microscopy techniques (22). To the best of our knowledge, this is the first investigation performed on colistin-heteroresistant *A. baumannii* strains using the surface imaging capabilities of the AFM.

Although the focus of this study was not on AFM methodology, validation of bacterial sample preparation procedures was crucial to ensure the surface depicted provided an accurate reflection of its true nature. Centrifugation and washing of bacterial cultures function to remove broth and bacterial debris; however, centrifugation speeds ranging from 1,000 × *g* (29) up to ~15,000 × *g* (3) (from investigations of *Staphylococcus epidermidis* and lactic acid bacteria, respectively), have

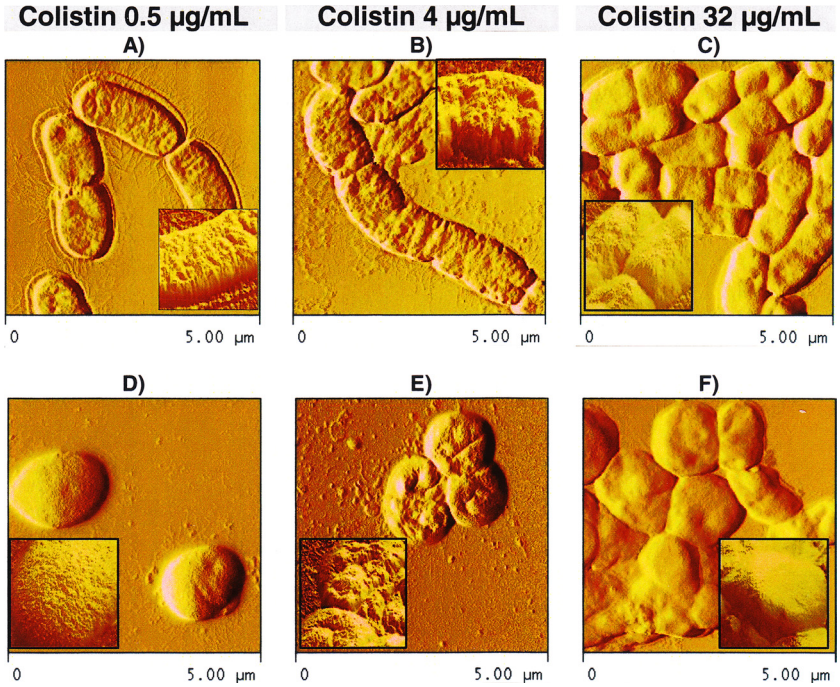

FIG. 4. AFM amplitude images and high-magnification surface three-dimensional plots (1 μm by 1 μm; reconstructed from height data) of mid-logarithmic-phase colistin-susceptible (A to C) and -resistant (D to F) *A. baumannii* ATCC 19606 cells treated for 20 min with colistin at 0.5 μg/ml (A and D), 4 μg/ml (B and E), and 32 μg/ml (C and F).

TABLE 2. Cellular dimensions and average RMS surface roughness of colistin-susceptible and -resistant (ATCC 19606 Col10) cells of *A. baumannii* ATCC 19606 at mid-logarithmic and stationary growth phases after colistin treatment

Growth phase and colistin concn	Susceptible			Resistant	
	Width (μm)	Length (μm)	Avg RMS surface roughness (nm)	Diam (μm)	Avg RMS surface roughness (nm)
Mid-log phase					
0.5 μg/ml	1.03 ± 0.09[a]	1.63 ± 0.24[a]	8.64 ± 2.4[b,c]	0.95 ± 0.21[a]	11.5 ± 2.1[b,c]
4 μg/ml	0.94 ± 0.06[a]	1.44 ± 0.17[a]	13.5 ± 5.6[b]	0.98 ± 0.09[a]	23.8 ± 5.2[b]
32 μg/ml	0.97 ± 0.07[a]	1.59 ± 0.23[a]	19.8 ± 4.3[b]	1.06 ± 0.11[a]	14.3 ± 4.1[b]
Stationary phase					
0.5 μg/ml	ND[d]	ND	7.81 ± 2.4[b,c]	ND	11.9 ± 2.8[b,c]
4 μg/ml	ND	ND	16.7 ± 4.7[b]	ND	26.1 ± 6.0[b]
32 μg/ml	ND	ND	15.3 ± 2.9[b]	ND	14.9 ± 2.9[b]

[a] Not significantly different from corresponding dimension following treatment at different colistin concentrations ($P > 0.05$).
[b] Significantly different following treatment at different colistin concentrations ($P < 0.05$).
[c] Not significantly different from untreated cells.
[d] ND, not determined due to marked morphological heterogeneity.

been employed for various durations to prepare bacterial samples. Considerable variability has been detected in the extent to which bacterial cells are altered by centrifugal shear forces; this encompasses changes to cellular viability (15), surface constituents (36), and surface properties (32) which may subsequently impede the interaction between antimicrobial agents and bacterial cells (15, 16). Additionally, the use of buffer to wash cells has led to the presence of a "fern-like matrix" surrounding the cells in AFM images, which was proposed to be derived from buffer salts (14). An appropriate protocol for the preparation of *A. baumannii* for AFM imaging which achieved adequate cleansing of the surface under minimal centrifugal conditions was thus determined to be two washes of bacterial culture with Milli-Q water at a centrifugal speed of 3,000 × *g* for 5 min (Fig. 1C).

Another significant point for consideration in bacterial characterization is the growth phase, as the development of surface macromolecules and cellular constituents is a dynamic process evolving over the entire growth of a bacterium and may therefore also influence bacterial surface properties (41). *A. baumannii* has been described to adopt a cocco-bacillar morphology (40) and was reported in coccus form at stationary growth phase (34). Interestingly, distinction in morphology at stationary phase was also noted here; however, unlike previous reports, the opposite trend of elongation was observed with cells extending up to ~18 μm in length for both colistin-susceptible (Fig. 2C) and colistin-resistant (Fig. 2F) cells. This phenomenon was more frequently observed in the susceptible population, although greater morphological heterogeneity was detected for stationary-phase resistant cells. Factors including bacterial nutrient status (22, 39) and desiccation (21) have been shown to influence the morphology of *A. baumannii* (21, 22). Additionally, elongated worm-like cells have been similarly observed in other gram-negative bacteria (e.g., *P. aeruginosa*, *Escherichia coli*, and *K. pneumoniae*) (7) in response to low concentrations of lomefloxacin (31) and β-lactam and sulfonamide antibiotics (7, 37). The exact mechanism of elongation detected in this investigation of *A. baumannii* is presently unknown, and its influence on decreased colistin susceptibility at stationary phase (33) requires further investigation.

Comparison between colistin-susceptible and -resistant subpopulations from AFM images illustrated a contrasting coccal morphology of resistant cells (Fig. 2D to F) in comparison to the susceptible cells (Fig. 2A to C), which adopted a bacillar shape. Additionally, differences in the surface topography (Fig. 3) were observed between susceptible and resistant cells; these were seen to be consistent across all growth phases. Although these differences in morphology and topography of colistin-resistant cells cannot directly account for colistin resistance in *A. baumannii*, the resistance mechanism may be related to structural differences in the outer membrane of each subpopulation. Our observations further contribute to recent findings that have highlighted a substantially increased susceptibility to several other antibiotics for colistin-resistant cells, including those to which *A. baumannii* strains are usually resistant (such as rifampin and macrolides) (25). Further comparison between colistin-susceptible and -resistant subpopulations revealed that the extracellular appendages surrounding colistin-resistant cells were shorter and less densely populated than those in colistin-susceptible cells. Lack of bacterial pili may account for negligible biofilm formation, which is supported by our observations of colistin-resistant *A. baumannii* (25).

A number of AFM time-course studies investigating the effects of antibiotics (5, 9, 44), including cyclic antimicrobial peptides (10, 24, 28, 35), on the bacterial surface have positively contributed to an understanding of the mechanisms of action of various antibiotics. Good correlation between the extent of outer membrane damage with increasing incubation time and antibiotic concentration has been established (10, 24, 28, 35). Similarly, colistin-induced disruption of the outer membrane of mid-logarithmic (Fig. 4) and stationary-phase (images not shown) *A. baumannii* cells illustrated that exposure to a sub-MIC colistin concentration (0.5 μg/ml) was sufficient to impart topographical changes to colistin-susceptible cells (Fig. 4A). These observations were consistent with results from static time-kill studies (27, 30), in which substantial killing occurred initially at sub-MIC colistin concentrations. Rapid concentration-dependent bacterial killing has been revealed at concentrations above the MIC (45); hence, the cells imaged following colistin treatment at these high concentrations pos-

sibly represent the most resistant subpopulation within each strain. At 4 μg/ml (2× to 4× the MIC), colistin caused substantial disruption of the outer membrane of both susceptible and resistant cells (reflected by roughness measurements in Table 2) without compromising the cell shape. Cell clustering and surface "smoothening" were observed for both strains upon exposure to 32 μg/ml colistin. It is likely that the root mean squared (RMS) roughness (RMS value of all surface height fluctuations from the mean surface height level) (8) was sensitive to the presence of large craters in the cell surface upon treatment with 32 μg/ml colistin, which may account for differences observed between numerical roughness measurements (19.8 ± 4.3 nm for susceptible cells versus 14.3 ± 4.1 nm for resistant cells) (Table 2) and the apparent cell surface smoothness (Fig. 2C and F). Although the increase in numerical surface roughness corresponded with increasing colistin concentrations for susceptible cells, this relationship was not detected for resistant cells (Table 2); the reasons for this are unknown. However, the observation that the surface of colistin-resistant cells responds in a similar manner to susceptible strains to treatment with various colistin concentrations (Fig. 2) is fascinating and suggests that the ability of colistin to interact with the outer membrane of resistant *A. baumannii* cells is maintained.

Interpretation of these AFM images requires consideration of the fact that this study was conducted under ambient conditions. A number of time-course microbial AFM imaging investigations have been similarly conducted in air (6, 12, 24, 28) as this enables high-resolution imaging. In this manner, drying small aliquots of prepared bacterial suspensions may impede an accurate illustration of the hydrated bacterial surface. It must be noted, however, that *A. baumannii* exhibits great resistance to desiccation and can survive for prolonged periods under dry conditions (20, 21, 42). Examination of the surface of *A. baumannii* in liquid is currently being undertaken.

In summary, this study is the first to differentiate between the morphology and topography of colistin-susceptible versus -resistant cells from heteroresistant *A. baumannii* strains at different growth phases and after colistin exposure. The contrasting spherical appearance of resistant cells was noted, in comparison to the rod-shaped susceptible cells. Resistant cells also displayed a finer surface topography, which was reflected by increased quantitative surface roughness in comparison to that of susceptible cells. Cellular elongation at stationary phase was apparent for both colistin-susceptible and -resistant strains, and levels of bacterial outer membrane damage observed in response to colistin exposure were similar for both strains. Investigations are warranted to elucidate the genetic mechanism(s) leading to such variations in morphology and topography, which will facilitate a comprehensive understanding of colistin resistance.

ACKNOWLEDGMENTS

We are sincerely grateful to Terri Camesano and her research team at Worcester Polytechnic Institute and Ruchi Yongsunthon for valuable advice regarding the technical operation of the AFM.

The work described was supported by Award no. R01AI079330 and Award no. R01AI070896 from the National Institute of Allergy and Infectious Diseases. This study was also partially supported by a grant from the Faculty of Pharmacy and Pharmaceutical Sciences, Monash University. J.L. is an Australian National Health and Medical Research Council R. Douglas Wright Research Fellow.

The content is solely the responsibility of the authors and does not necessarily represent the official views of the National Institute of Allergy and Infectious Diseases or the National Institutes of Health.

REFERENCES

1. **Abraham, T., S. R. Schooling, M. P. Nieh, N. Kucerka, T. J. Beveridge, and J. Katsaras.** 2007. Neutron diffraction study of Pseudomonas aeruginosa lipopolysaccharide bilayers. J. Phys. Chem. B **111:**2477–2483.
2. **Bergogne-Bérézin, E., and K. J. Towner.** 1996. *Acinetobacter* spp. as nosocomial pathogens: microbiological, clinical, and epidemiological features. Clin. Microbiol. Rev. **9:**148–165.
3. **Boonaert, C. J. P., and P. G. Rouxhet.** 2000. Surface of lactic acid bacteria: relationships between chemical composition and physicochemical properties. Appl. Environ. Microbiol. **66:**2548–2554.
4. **Boucher, H. W., G. H. Talbot, J. S. Bradley, J. E. Edwards, D. Gilbert, L. B. Rice, M. Scheld, B. Spellberg, and J. Bartlett.** 2009. Bad bugs, no drugs: no ESKAPE! An update from the Infectious Diseases Society of America. Clin. Infect. Dis. **48:**1–12.
5. **Braga, P. C., and D. Ricci.** 1998. Atomic force microscopy: application to investigation of *Escherichia coli* morphology before and after exposure to cefodizime. Antimicrob. Agents Chemother. **42:**18–22.
6. **Braga, P. C., and D. Ricci.** 2002. Differences in the susceptibility of Streptococcus pyogenes to rokitamycin and erythromycin A revealed by morphostructural atomic force microscopy. J. Antimicrob. Chemother. **50:**457–460.
7. **Catlin, B. W.** 1975. Cellular elongation under the influence of antibacterial agents: way to differentiate coccobacilli from cocci. J. Clin. Microbiol. **1:**102–105.
8. **Chen, Y., and W. Huang.** 2009. Influences of geometrical factors on quantitative surface roughness evaluations by atomic force microscopy. J. Nanosci. Nanotechnol. **9:**893–896.
9. **Chen, Z. Y., X. P. Guo, J. Y. Huang, Y. L. Hong, and Q. Zhang.** 2006. AFM study of the effect of metronidazole on surface structures of sulfate-reducing bacteria. Anaerobe **12:**106–109.
10. **da Silva, A., Jr., and O. Teschke.** 2003. Effects of the antimicrobial peptide PGLa on live Escherichia coli. Biochim. Biophys. Acta **1643:**95–103.
11. **Dufrene, Y. F.** 2004. Using nanotechniques to explore microbial surfaces. Nat. Rev. Microbiol. **2:**451–460.
12. **Eaton, P., J. C. Fernandes, E. Pereira, M. E. Pintado, and F. Xavier Malcata.** 2008. Atomic force microscopy study of the antibacterial effects of chitosans on Escherichia coli and Staphylococcus aureus. Ultramicroscopy **108:**1128–1134.
13. **Evans, M. E., D. J. Feola, and R. P. Rapp.** 1999. Polymyxin B sulfate and colistin: old antibiotics for emerging multiresistant gram-negative bacteria. Ann. Pharmacother. **33:**960–967.
14. **Gallardo-Moreno, A. M., Y. Liu, M. L. Gonzalez-Martin, and T. A. Camesano.** 2006. Atomic force microscopy analysis of bacterial surface morphology before and after cell washing. J. Scanning Probe Microsc. **1:**63–73.
15. **Gilbert, P., F. Coplan, and M. R. Brown.** 1991. Centrifugation injury of gram-negative bacteria. J. Antimicrob. Chemother. **27:**550–551.
16. **Gilbert, P., D. Pemberton, and D. E. Wilkinson.** 1990. Synergism within polyhexamethylene biguanide biocide formulations. J. Appl. Bacteriol. **69:**593–598.
17. **Grasso, D., B. F. Smets, K. A. Strevett, B. D. Machinist, C. J. van Oss, R. F. Giese, and W. Wu.** 1996. Impact of physiological state on surface thermodynamics and adhesion of Pseudomonas aeruginosa. Environ. Sci. Technol. **30:**3604–3608.
18. **Hancock, R. E. W.** 1997. Peptide antibiotics. Lancet **349:**418–422.
19. **Hawley, J. S., C. K. Murray, and J. H. Jorgensen.** 2008. Colistin heteroresistance in *Acinetobacter* and its association with previous colistin therapy. Antimicrob. Agents Chemother. **52:**351–352.
20. **Hirai, Y.** 1991. Survival of bacteria under dry conditions from a view point of nosocomial infection. J. Hosp. Infect. **19:**191–200.
21. **Houang, E. T., R. T. Sormunen, L. Lai, C. Y. Chan, and A. S. Leong.** 1998. Effect of desiccation on the ultrastructural appearances of Acinetobacter baumannii and Acinetobacter lwoffii. J. Clin. Pathol. **51:**786–788.
22. **James, G. A., D. R. Korber, D. E. Caldwell, and J. W. Costerton.** 1995. Digital image analysis of growth and starvation responses of a surface-colonizing *Acinetobacter* sp. J. Bacteriol. **177:**907–915.
23. **Landman, D., C. Georgescu, D. A. Martin, and J. Quale.** 2008. Polymyxins revisited. Clin. Microbiol. Rev. **21:**449–465.
24. **Li, A., P. Y. Lee, B. Ho, J. L. Ding, and C. T. Lim.** 2007. Atomic force microscopy study of the antimicrobial action of Sushi peptides on Gram negative bacteria. Biochim. Biophys. Acta **1768:**411–418.
25. **Li, J., R. L. Nation, R. J. Owen, S. Wong, D. Spelman, and C. Franklin.** 2007. Antibiograms of multidrug-resistant clinical Acinetobacter baumannii: promising therapeutic options for treatment of infection with colistin-resistant strains. Clin. Infect. Dis. **45:**594–598.
26. **Li, J., R. L. Nation, J. D. Turnidge, R. W. Milne, K. Coulthard, C. R. Rayner,**

and D. L. Paterson. 2006. Colistin: the re-emerging antibiotic for multidrug-resistant Gram-negative bacterial infections. Lancet Infect. Dis. **6:**589–601.
27. **Li, J., C. R. Rayner, R. L. Nation, R. J. Owen, D. Spelman, K. E. Tan, and L. Liolios.** 2006. Heteroresistance to colistin in multidrug-resistant *Acinetobacter baumannii*. Antimicrob. Agents Chemother. **50:**2946–2950.
28. **Meincken, M., D. L. Holroyd, and M. Rautenbach.** 2005. Atomic force microscopy study of the effect of antimicrobial peptides on the cell envelope of *Escherichia coli*. Antimicrob. Agents Chemother. **49:**4085–4092.
29. **Mendez-Vilas, A., A. M. Gallardo-Moreno, and M. L. Gonzalez-Martin.** 2007. Atomic force microscopy of mechanically trapped bacterial cells. Microsc. Microanal. **13:**55–64.
30. **Owen, R. J., J. Li, R. L. Nation, and D. Spelman.** 2007. In vitro pharmacodynamics of colistin against Acinetobacter baumannii clinical isolates. J. Antimicrob. Chemother. **59:**473–477.
31. **Padieskaya, E. N., and L. F. Stebaeva.** 1995. The effect of lomefloxacin on morphology and ultrastructure of the cells of Gram-negative bacteria. Farm. Zh. **29:**13–16.
32. **Pembrey, R. S., K. C. Marshall, and R. P. Schneider.** 1999. Cell surface analysis techniques: what do cell preparation protocols do to cell surface properties? Appl. Environ. Microbiol. **65:**2877–2894.
33. **Poudyal, A., R. J. Owen, J. B. Bulitta, A. Forrest, B. T. Tsuji, J. D. Turnidge, D. Spelman, B. P. Howden, R. L. Nation, and J. Li.** 2008. High initial inocula and stationary growth phase substantially attenuate killing of *Klebsiella pneumoniae* and *Acinetobacter baumannii* by colistin, abstr. A-1673, p. 28. Abstr. 48th Annu. Intersci. Conf. Antimicrob. Agents Chemother. (ICAAC)-Infect. Dis. Soc. Am. (IDSA) 46th Annu. Meet. American Society for Microbiology and Infectious Diseases Society of America, Washington, DC.
34. **Public Health Image Library.** 2009. *Acinetobacter baumannii*. Public Health Image Library, Centers for Disease Control and Prevention, Atlanta, GA. http://phil.cdc.gov/phil/home.asp. Accessed 5 August 2009.
35. **Rossetto, G., P. Bergese, P. Colombi, L. E. Depero, A. Giuliani, S. F. Nicoletto, and G. Pirri.** 2007. Atomic force microscopy evaluation of the effects of a novel antimicrobial multimeric peptide on Pseudomonas aeruginosa. Nanomedicine **3:**198–207.
36. **Smets, B. F., D. Grasso, M. A. Engwall, and B. J. Machinist.** 1999. Surface physicochemical properties of Pseudomonas fluorescens and impact on adhesion and transport through porous media. Colloids Surf. B Biointerfaces **14:**121–139.
37. **Takahashi, M., Y. Ichiman, E. Yoshida, C. Sasaki, and Y. Yonaha.** 1988. Effect of antibiotics on the adsorption of Klebsiella pneumoniae to cultured cells. Chemotherapy (Tokyo) **36:**779–786.
38. **Tan, C.-H., J. Li, and R. L. Nation.** 2007. Activity of colistin against heteroresistant *Acinetobacter baumannii* and emergence of resistance in an in vitro pharmacokinetic/pharmacodynamic model. Antimicrob. Agents Chemother. **51:**3413–3415.
39. **Tomaras, A. P., M. J. Flagler, C. W. Dorsey, J. A. Gaddy, and L. A. Actis.** 2008. Characterization of a two-component regulatory system from Acinetobacter baumannii that controls biofilm formation and cellular morphology. Microbiology **154:**3398–3409.
40. **von Graevenitz, A.** 1995. *Acinetobacter*, *Alcaligenes*, *Moraxella*, and other nonfermentative gram-negative bacteria, p. 520–532. *In* P. R. Murray, E. J. Baron, M. A. Pfaller, F. C. Tenover, and R. H. Yolken (ed.), Manual of clinical microbiology, 6th ed. ASM Press, Washington, DC.
41. **Walker, S. L., J. E. Hill, J. A. Redman, and M. Elimelech.** 2005. Influence of growth phase on adhesion kinetics of *Escherichia coli* D21g. Appl. Environ. Microbiol. **71:**3093–3099.
42. **Wendt, C., B. Dietze, and E. Deitz.** 1997. Survival of *Acinetobacter baumannii* on dry surfaces. J. Clin. Microbiol. **35:**1394–1397.
43. **West, P., and A. Ross.** 2006. An introduction to atomic force microscopy modes. Pacific Nanotechnology, Inc., Irvine, CA.
44. **Yang, L., K. Wang, W. Tan, X. He, R. Jin, J. Li, and H. Li.** 2006. Atomic force microscopy study of different effects of natural and semisynthetic beta-lactam on the cell envelope of Escherichia coli. Anal. Chem. **78:**7341–7345.
45. **Yau, W., R. J. Owen, A. Poudyal, J. M. Bell, J. D. Turnidge, H. H. Yu, R. L. Nation, and J. Li.** 2008. Colistin hetero-resistance in multidrug-resistant Acinetobacter baumannii clinical isolates from the Western Pacific region in the SENTRY antimicrobial surveillance programme. J. Infect. **58:**138–144.
46. **Zavascki, A. P., L. Z. Goldani, J. Li, and R. L. Nation.** 2007. Polymyxin B for the treatment of multidrug-resistant pathogens: a critical review. J. Antimicrob. Chemother. **60:**1206–1215.